Asymptotically Stable Gait Primitives for Planning Dynamic Bipedal Locomotion in Three Dimensions

Robert D. Gregg, Timothy Bretl, and Mark W. Spong

Abstract— **This paper applies geometric reduction-based control to derive a set of asymptotically stable dynamic walking gaits for a 3-D bipedal robot, each corresponding to walking along a nominal arc of constant curvature for a fixed number of steps. We show that any such set of *asymptotically stable gait primitives* may be composed in arbitrary order without causing the robot to fall, so any walking path that is a sequence of these gaits may be followed by the robot. This result enables motion planning for bipedal dynamic walkers, which are *fast* and *energetically efficient*, in a similar manner to what is already possible for biped locomotion based on Zero Moment Point (ZMP) equilibrium constraints.**

I. Introduction

The step-level mechanics and high-level motion planning of humanoid walking have been active areas of research over the past decades. The incredible efficiency of bipedalism, which allows humans to outwalk quadrupeds over long distances [20], motivates its use on locomotive mechanisms. In fact, researchers have demonstrated "passive dynamic" walking down shallow slopes for simple planar biped models without any actuation whatsoever [8], [23].

This energy-efficient form of locomotion, known as *dynamic walking*, is based on "controlled falling," where each step cycle involves a gravity-powered pendular fall towards the ground, until foot impact transfers this natural falling motion to the other leg. In terms of a walker's joint trajectories, this produces attractive periodic orbits called *limit cycles*. Hobbelen and Wisse offer a useful definition of this in [13]:

> *Limit cycle [i.e., dynamic] walking is a nominally periodic sequence of steps that is stable as a whole but not locally stable at every instant in time.*

Many sophisticated humanoid robots, such as HRP-2 and Honda ASIMO, have demonstrated robotic bipedal locomotion. However, the motion of these robots is constrained by "quasi-static" equilibrium conditions related to the Zero Moment Point (ZMP), which produces walking that is *not* dynamic according to the above definition. Recall that a walking mechanism compensates for gravity by applying forces against the ground, resulting in a reaction force acting at a point known as the Center of Pressure (CoP). In order to remain statically balanced, there must be zero net moment at the CoP, and this so-called Zero Moment Point (ZMP) must be within the biped's support polygon, e.g., the convex hull of the ground contact area(s). When the Zero Moment Point exits the support polygon, the biped rotates about a new passive degree-of-freedom (DOF) at the edge of a stance foot. This falling scenario is always avoided by ZMP motion planners, whereas dynamic walking gaits are largely composed of such pendular falling states.

In order to constrain walking trajectories for ZMP motion, large actuators must track joint angles/velocities while actively supporting the body weight with flexed knees during the entirety of each step cycle [13], [18]. This results in unnatural shuffling motion that is up to an order of magnitude *less efficient* than dynamic walking in terms of specific energetic cost of transport (energy consumed per unit weight per unit distance) [4]. Arguably, ZMP gaits may have a closer resemblance to the inefficient postural attributes of chimpanzee bipedalism – these hunched gaits similarly have flexed knees that never pass beneath the hip joint, preventing the pendular falling motion of dynamic walking gaits [27].

However, ZMP methods have proved useful in many motion planning studies, allowing locomotion with obstacle avoidance in three-dimensional (3-D) space [31], interaction with the environment [15], [16], and walking and climbing on rough terrain [12]. Although step-level motion planning over irregular terrain has also been applied to planar dynamic walkers [22], [24], we are unaware of any *path planning* results for dynamic walking in 3-D space. This is likely due to the difficulty in finding stable dynamic gaits for 3-D bipedal robots, where complex dynamics must be controlled to produce asymptotically stable limit cycles without canceling the beneficial passive dynamics that are fundamental to efficient bipedalism.

Work towards 3-D dynamic walking began with models of the sagittal and frontal planes-of-motion (without heading, see Fig. 1), resulting in spatially 3-D dynamic gaits (e.g., [2], [17], [26]). However, work on fully 3-D (i.e., directional) dynamic walking is limited, with some of the earliest theoretical results presented in [9]–[11]. In these papers, geometric *reduction-based control* is employed to build 3-D gaits about arbitrary headings, based on subsystem limit cycles in the sagittal plane-of-motion (where bilateral symmetry yields periodic motion from step to step). Rigorous results for underactuated 3-D bipeds are presented in [25], where virtual constraints are enforced to restrict analysis to the periodic motion of a reduced-order subsystem. Both methods demonstrate steering capabilities, with the latter showing stability for steering along paths with mild curvature.

In order to build bipedal robots that can quickly and

R. D. Gregg is with the Department of Electrical and Computer Engineering, and T. Bretl is with the Department of Aerospace Engineering, University of Illinois at Urbana-Champaign, Urbana, IL 61801 {rgregg,tbretl}@illinois.edu

M. W. Spong is with the Department of Electrical Engineering, University of Texas at Dallas, Richardson, TX 75080 mspong@utdallas.edu

This research was partially supported by NSF Grant CMMI-0856368.

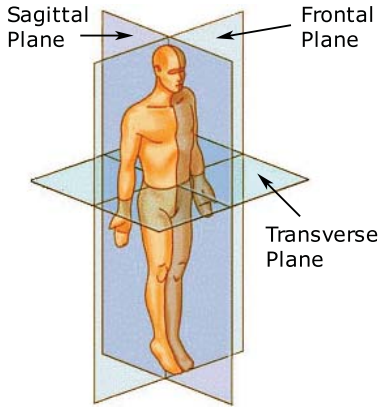

Fig. 1. The transverse (or axial), frontal (or lateral), and sagittal planes-of-motion of the human body [30]. These correspond to the yaw/heading, lean/roll, and pitch degrees-of-freedom, respectively, at the foot.

efficiently navigate through real-world environments, the stability of dynamic walking must be considered when *planning* walking paths with significant steering. This is no trivial task, as turning motion inherently deviates from known stable limit cycles associated with straight-ahead walking [9]. Unlike ZMP methods, the robot state cannot be checked against closed-form balance constraints. The hybrid nonlinear dynamics of a dynamic walker make it difficult to analytically assure stability – the fate of a walking trajectory from given initial conditions is usually computed in simulation [8].

Therefore, we present a theoretical framework for building stable walking paths for dynamic walking bipeds. We show that straight-ahead and turning gaits form a set of motion primitives that enable motion planning techniques, commonly used on ZMP walkers, to be applied to dynamic walkers. We survey related work in Section II, followed by an overview of dynamic walking and stability in Section III. Here we describe an example 3-D "compass-gait" biped and its reduction-based controller. We introduce and demonstrate the notion of gait primitives in Section IV. Our main theoretical result is presented in Section V, where we derive the rules for composing gait primitives. We then formulate the path planning problem in Section VI, followed by numerical results in Section VII and closing remarks in Section VIII.

II. Related Work

We now discuss some stability results in dynamic motion control, followed by motivating work in humanoid path planning based on postural ZMP constraints. Note the important distinction that satisfying the ZMP condition does not necessarily imply stable walking motion [29, Section 10.8].

A. Stable Dynamic Motion Control

Geometric methods are used in [11] to construct 3-D straight-ahead walking gaits corresponding to locally exponentially stable (LES) limit cycles, i.e., local asymptotic stability (LAS) with exponentially fast convergence. This paper's steering results are extended in [9], [10], showing that constant-curvature steering between steps induces LES limit cycles corresponding to circular turning. However, walking paths can entail an *arbitrary* sequence of turning motions that may accumulate perturbations and lead to instability.

Virtual constraints are used in [25] to construct LES straight-ahead gaits, which can be stably steered towards nearby headings. In particular, LAS implies local input-to-state stability: sufficiently small changes in heading result in small changes in state between impact events. However, it is difficult to deduce the bounds for this form of stability over a curved walking path (i.e., what range of initial states will recover from some bounded sequence of steering angles).

The present paper intends to show that different LAS gaits can be sequentially composed to build stable walking paths. This is directly related to the switching controller-composition method of [3], where (Lyapunov) funnels show stability for sequential paddle-and-ball batting maneuvers.

B. ZMP Motion Planners

Full-body posture planning is achieved in [16] by initially computing a large set of statically-stable configurations. A path between goal configurations is then found by growing a rapidly-exploring random tree, which connects samples only if a collision-free ZMP-constrained path exists. This is used in [15] for locomotion planning, restricting the problem to a discrete set of foot placements connected by valid stepping motions. A similar method in [12] pre-computes a small set of ZMP-constrained *motion primitives*, which bias the sampling of configurations between planned foot placements. These primitives prescribe high-quality motions that can be shaped to match common tasks such as walking and climbing. Instead of tracking pre-computed trajectories, our approach is based on asymptotically stable limit cycles.

A two-stage global planner is proposed in [31] that first uses a sampling-based algorithm to find a collision-free path for the *functional decomposition* of the robot body. That is, the robot is modeled as a bounding box on a walking surface, reducing the initial planning problem to configuration space $SE(2)$ (x, y, and orientation). Randomly generated samples are locally connected by *Dubins curves* (circular arcs with tangential line segments [6]), and these $SE(2)$ paths are given to a walking pattern generator that produces constrained whole-body motions for ZMP-constrained locomotion. We will show that the nature of our gait primitives allows a similar functional decomposition approach for generating stable dynamic walking paths composed of constant-curvature arc segments.

III. Dynamic Walker Model

A bipedal robot can be modeled as a hybrid system, which contains both continuous and discrete dynamics. We assume full actuation at the stance ankle of flat feet, which have instantaneous and perfectly plastic impact events. During the continuous swing phase, the contact between stance foot and ground is assumed flat without slipping. Note that some of these assumptions can be relaxed as in [25], [26]. We begin with some formalisms for hybrid systems from [2], [29].

A. Hybrid Systems

Since knee-lock impacts introduce another level of complexity to the hybrid model, we only consider discrete events associated with foot-ground impacts (which does not preclude knees without impacts [29]). We therefore define hybrid models with one continuous phase, i.e., "systems with impulse effects." A *hybrid control system* has the form

$$\mathscr{HC} : \begin{cases} \dot{x} = f(x) + g(x)u & x \in D \backslash G \\ x^+ = \Delta(x^-) & x^- \in G \end{cases},$$

where $G \subset D$ is called the *guard* and $\Delta : G \to D$ is the *reset map*. A *hybrid system* $\mathscr{H}$ is a hybrid control system without an explicit control input u (e.g., a closed-loop system), and a *hybrid flow* is a solution curve to a hybrid system [2].

We must define periodicity, since bipedal walking gaits typically repeat every two steps due to bilateral symmetry in the sagittal plane and side-to-side swaying motion in the other planes. In the case of simple models without hip links, there is no swaying motion outside of the sagittal plane, so each leg has an identical swing phase that repeats every step [9]. Since a biped's dynamics are described by a hybrid system, a walking gait that is h-step periodic corresponds to an *h-periodic* hybrid flow $x(t)$, such that $x(t) = x(t + \sum_{i=1}^{h} T_i)$, for all $t \geq 0$, where T_i is the fixed *time-to-impact* between the $(i-1)^{th}$ and i^{th} discrete events. The time-invariant geometry of such a solution is characterized by the *h-periodic hybrid orbit* $\mathcal{O} = \{x(t) | t \geq 0\} \subset D$ from [29].

The stability of periodic hybrid orbits (i.e., limit cycles) is determined by studying the *Poincaré map* $P : G \to G$, as done in [2], [29]. This is a discrete map defined on the *Poincaré section*, naturally chosen to be guard G, which characterizes the evolution of a hybrid flow between intersections with G. In particular, the h-composition of this map sends state $x_j \in G$ ahead h impact events by the discrete system $x_{j+h} = P^h(x_j)$. In the case of a h-periodic hybrid orbit $\mathcal{O}$, we have a *h-fixed-point* $x^* \in G \cap \mathcal{O}$ such that $x^* = P^h(x^*)$. Although we cannot analytically calculate this map to determine its stability about x^*, we can numerically approximate it through simulation. This allows us to analyze orbit stability as a linear discrete system by the map's linearization, δP^h. We then know that a periodic hybrid orbit is *locally exponentially stable* (LES) if and only if the eigenvalue magnitudes of δP^h are strictly within the unit circle. The local stability region about h-fixed-point x^*, known as the *basin of attraction*, is defined as

$$BoA(x^*) = \{x \in G \text{ s.t. } \lim_{z \to \infty} P^{hz}(x) = x^*\}. \quad (1)$$

We defer the numerical details of Poincaré analysis to [8].

B. Biped Dynamics

For the sake of clarity, we adopt a 3-D extension of the commonly studied planar compass-gait biped shown in Fig. 2. This simple 4-DOF biped has no hip link, but we could similarly apply this paper's concepts to more complex models with hips and splayed legs as in [10], [11]. We now describe our biped's hybrid control system $\mathscr{HC}_{4\mathrm{D}}$.

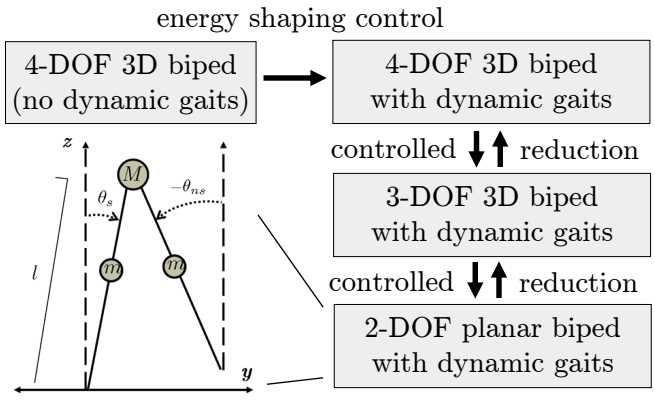

Fig. 2. Controlled reduction overview: the first reduction stage divides out the yaw DOF of the transverse plane, and the second stage divides out the lean DOF of the frontal plane, yielding the dynamics of the planar biped.

We represent the configuration space of this biped by $Q = \mathbb{T}^4$ with coordinates $q = (\psi, \varphi, \theta^T)^T$, where ψ is the yaw (or heading), φ is the roll (or lean) from vertical, and $\theta = (\theta_{\mathrm{s}}, \theta_{\mathrm{ns}})^T$ is the vector of sagittal-plane (pitch) variables as in the associated 2-D model. The biped's continuous dynamics can be derived using Lagrangian mechanics, starting with state $x = (q^T, \dot{q}^T)^T$ in phase space TQ (configurations and tangent velocities). We then define the Lagrangian function in terms of the robot's kinetic and potential energies:

$$\mathcal{L}(q, \dot{q}) = \mathcal{K}(q, \dot{q}) - \mathcal{V}(q) = \tfrac{1}{2}\dot{q}^T M(q)\dot{q} - \mathcal{V}(q), \quad (2)$$

where the kinetic energy depends on 4×4 inertia/mass matrix

$$M(\varphi, \theta) = \begin{pmatrix} m_\psi(\varphi, \theta) & \multicolumn{2}{c}{\multirow{2}{*}{——}} & M_{\psi,\varphi,\theta}(\varphi, \theta) \\ | & & & M_{\varphi,\theta}(\theta) \\ M^T_{\psi,\varphi,\theta}(\varphi, \theta) & \multicolumn{2}{c}{M^T_{\varphi,\theta}(\theta)} & M_\theta(\theta) \end{pmatrix} \begin{matrix} \\ m_\varphi(\theta) \\ \\ \end{matrix}.$$

The potential energy $\mathcal{V}(\varphi, \theta) = \mathcal{V}_\theta(\theta)\cos(\varphi)$ contains the planar subsystem potential energy $\mathcal{V}_\theta$.

This function satisfies the Euler-Lagrange (E-L) equations

$$\tfrac{d}{dt}\nabla_{\dot{q}}\mathcal{L} - \nabla_q \mathcal{L} = Bu, \quad (3)$$

giving the dynamics of the controlled robot:

$$M(q)\ddot{q} + C(q, \dot{q})\dot{q} + N(q) = Bu, \quad (4)$$

where 4×4-matrix C contains the Coriolis/centrifugal terms, $N = \nabla_q \mathcal{V}$ is the vector of potential torques, and 4×4-matrix B is assumed invertible for full actuation. Moreover, control input u is the vector of joint torques, subject to actuator saturation at torque constant U^{max}.

In order to model walking on a flat surface, we take domain $D \subset TQ$ to be the set of states with nonnegative swing foot height. Impact events are triggered when this height is zero and decreasing, characterized by guard $G \subset D$ and impact map Δ. In the simulations throughout this paper, we adopt common physical parameters from the literature: M = 10 kg, m = 5 kg, l = 1 m, U^{max} = 20 Nm. More detail on our model, including expressions for its symbolic terms, is provided in [11].

C. Reduction-Based Control

A geometric property of open-chain robots was introduced in [9], [11], identifying extensive symmetries in robot dynamics. Reduction-based control exploits these symmetries to decompose robot dynamics into lower-dimensional control problems. Using control to shape the energy of an n-DOF robot, the shaped dynamics can be projected onto the dynamics of a corresponding m-DOF "subrobot". This subsystem is entirely decoupled from the first $k = n - m$ coordinates and thus behaves and can be controlled as a typical m-DOF robot. The first k DOF evolve according to controlled momentum equations yielding stabilized set-points or periodic orbits.

In the context of bipedal walking, controlled reduction first separates the transverse plane-of-motion to control yaw to desired heading $\bar{\psi}$, then separates the frontal plane-of-motion to stabilize lean about vertical. Given this controlled reduction to the sagittal-plane subsystem defined on reduced-order phase space TQ modulo $T\mathbb{T}^2$, we can find limit cycles in the dynamics of the planar biped associated with Lagrangian $\mathcal{L}_\theta(\theta, \dot{\theta}) = \frac{1}{2}\dot{\theta}^T M_\theta(\theta)\dot{\theta} - \mathcal{V}_\theta$. The control law that enables this controlled reduction is depicted in Fig. 2, but due to space constraints we refer the reader to [9], [11] for details.

This method allows us to build full-order 3-D dynamic walking gaits, leading to our discussion on gait primitives.

IV. Generating Gait Primitives

In this section, we discuss creating our set of asymptotically stable gait primitives corresponding to strategies for both straight-ahead walking and left/right turning. These strategies enable motion planning for the biped, which chooses a gait from this set for every step cycle. We will later discuss rules for stably switching between different gaits. To begin, we formalize the notion of gait primitives.

Definition 1: An *asymptotically stable gait primitive* is a pair $\mathcal{G} = (\mathscr{H}^{\mathrm{cl}}, x^*)$, where $\mathscr{H}^{\mathrm{cl}}$ is a closed-loop hybrid system of a controlled biped, and x^* is an asymptotically stable fixed-point (modulo heading change) of $\mathscr{H}^{\mathrm{cl}}$.

Since asymptotically stable limit cycles are fundamental to dynamic walking, we often call these *dynamic* gait primitives for brevity. Recall that our example 4-DOF biped has no hip, so we will find 1-step periodic gaits. We now derive this biped's gait primitives, but note that this paper's planning framework pertains to any set of asymptotically stable gaits (not necessarily from our reduction-based control method).

A. Straight-Ahead Gait Primitive

The reduction-based control law of Fig. 2 yields closed-loop hybrid system $\mathscr{H}^{\mathrm{st}}_{4\mathrm{D}}$ for straight-ahead walking on flat ground. For our example, we set $\bar{\psi} = 0$ without loss of generality, finding the 1-fixed-point $x^{*\mathrm{st}}_{4\mathrm{D}}$ given in (5). We numerically verify LES of this straight-ahead gait by linearizing the associated Poincaré map P_{st}, and we denote the basin of attraction as $BoA_{\mathrm{st}}(x^{*\mathrm{st}}_{4\mathrm{D}})$. This defines the *straight-ahead* gait primitive $\mathcal{G}^{\mathrm{st}}_{4\mathrm{D}} = (\mathscr{H}^{\mathrm{st}}_{4\mathrm{D}}, x^{*\mathrm{st}}_{4\mathrm{D}})$.

The associated hybrid periodic orbit $\mathcal{O}^{\mathrm{st}}_{4\mathrm{D}}$ is illustrated in the plots of Fig. 3, showing its periodicity over one step. We see that this upright gait has no swaying in lean or yaw (which is to be expected for a hipless biped), but the sagittal plane has a periodic step length of 0.53 m and an approximate linear velocity of 0.73 m/s.

B. Turning Gait Primitive

We create turning gaits by introducing a periodic disturbance into $\mathscr{H}^{\mathrm{st}}_{4\mathrm{D}}$ in the form of constant steering between steps. In particular, we augment the within-stride reduction-based controller with an event-based (or stride-to-stride) controller that increments desired yaw $\bar{\psi}$ at each step by steering angle $s = \Delta\bar{\psi}$ (positive for clockwise or negative for counter-clockwise steering). This yields closed-loop system $\mathscr{H}^{\mathrm{tu}(s)}_{4\mathrm{D}}$, for which trajectories converge to 1-step periodic turning gaits modulo heading change s, where CW and CCW gaits are symmetric with opposite yaw/lean. We want to show that for any sufficiently small $|s|$, constant-curvature turning induces a LES 1-fixed-point modulo heading change:

$$(\psi^{*\mathrm{tu}(s)} + s, \varphi^{*\mathrm{tu}(s)}, \theta^{*\mathrm{tu}(s)^T}, \dot{q}^{*\mathrm{tu}(s)^T})^T = P_{\mathrm{tu}(s)}(x^{*\mathrm{tu}(s)})$$

with $BoA_{\mathrm{tu}(s)}(x^{*\mathrm{tu}(s)})$. We can then define *CW-turning* and *CCW-turning* gait primitives $\mathcal{G}^{\mathrm{tu}(s)}_{4\mathrm{D}}$ and $\mathcal{G}^{\mathrm{tu}(-s)}_{4\mathrm{D}}$.

Starting our biped's augmented system from $x^{*\mathrm{st}}_{4\mathrm{D}}$, we observe that hybrid flows converge to a 1-fixed-point $x^{*\mathrm{tu}(s)}_{4\mathrm{D}}$ associated with $\mathcal{O}^{\mathrm{tu}(s)}_{4\mathrm{D}}$ for any choice of $s \in [-S, S]$, $S = 0.492$. We densely sample steering values in $[-S, S]$, finding the fixed-point for each sample and confirming LES. The evolution of the fixed-point is plotted in Fig. 4. This also shows that periodic step length (and time duration) changes slowly as $|s|$ increases, which perturbs the sagittal-plane orbits compared to $\mathcal{O}^{*\mathrm{st}}_{4\mathrm{D}}$. Increasing $|s|$ into the instability region outside $[-S, S]$, we observe period-doubling (flip) bifurcations yielding 2- and 4-step periodic LES orbits, ultimately leading to a chaotic strange attractor and falling.

We demonstrate a CW and CCW turning gait by choosing $\hat{s} = 0.483$, which corresponds to the fixed-points in (6)-(7). The CW-turning gait is illustrated in Fig. 5 (and CCW by symmetry), which shows the gait's natural leaning into the turn. Finally, we emphasize that these turning gaits naturally arise from our asymptotically stable straight-ahead system, without changing any reference trajectories.

C. Orienting Primitives

Recall that we derived each of these primitives from heading $\psi = 0$. Our closed-loop biped can be arbitrarily oriented about the z-axis for walking along any heading:

Proposition 1: If gait primitive $\mathcal{G} = (\mathscr{H}^{\mathrm{cl}}_{\bar{\psi}_i}, x^*_{\psi_i})$ with initial ψ_i and $\bar{\psi}_i$ has LES fixed-point (modulo $s = \Delta\bar{\psi}$)

$$x^*_{\psi_i} := \left(q^{*^T}_{\psi_i}, \dot{q}^{*^T}\right)^T = \left(\psi_i, \varphi^*, \theta^{*^T}, \dot{q}^{*^T}\right)^T,$$

then $\mathcal{G} = (\mathscr{H}^{\mathrm{cl}}_{\bar{\psi}_j}, x^*_{\psi_j})$ is the same gait primitive with initial ψ_j and $\bar{\psi}_j = \bar{\psi}_i + (\psi_j - \psi_i)$, with LES fixed-point $x^*_{\psi_j}$.

Each primitive's closed-loop hybrid system is *autonomous* (no reference trajectories) and thus invariant with respect to time. Therefore, a general set of asymptotically stable

$$x_{4\mathrm{D}}^{*\mathrm{st}} \approx (0, 0, -0.2704, 0.2704, 0, 0, -1.4896, -1.7986)^T \quad (5)$$

$$x_{4\mathrm{D}}^{*\mathrm{tu}(\hat{s})} \approx (-0.0306, -0.0064, -0.2782, 0.2782, -0.0318, 0.0159, -1.5426, -2.1318)^T \quad (6)$$

$$x_{4\mathrm{D}}^{*\mathrm{tu}(-\hat{s})} \approx (0.0306, 0.0064, -0.2782, 0.2782, 0.0318, -0.0159, -1.5426, -2.1318)^T \quad (7)$$

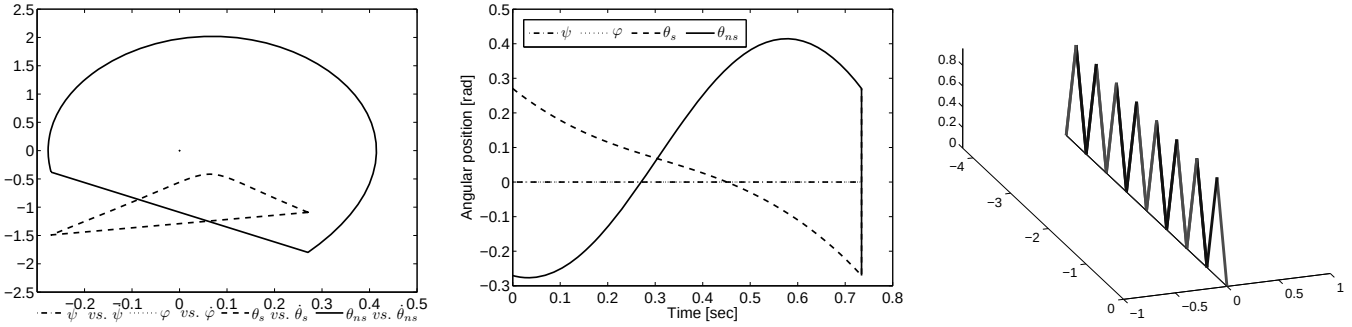

Fig. 3. Straight-ahead 1-step gait: phase portrait (left), coordinate trajectories (center), and multi-step visualization (right). The phase portrait shows planar slices of $\mathcal{O}_{4\mathrm{D}}^{st}$ by plotting angular positions against angular velocities, which we use to illustrate 1-step periodicity in phase space.

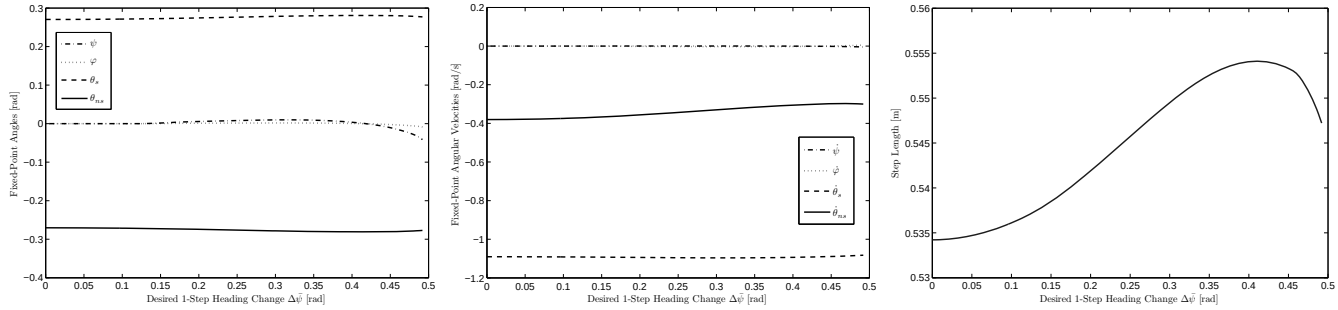

Fig. 4. Evolution of CW turning fixed-point $x_{4\mathrm{D}}^{*\mathrm{tu}(|s|)}$ angles (left), velocities (center), and associated step length (right) over steering angle $s = \Delta\bar{\psi}$.

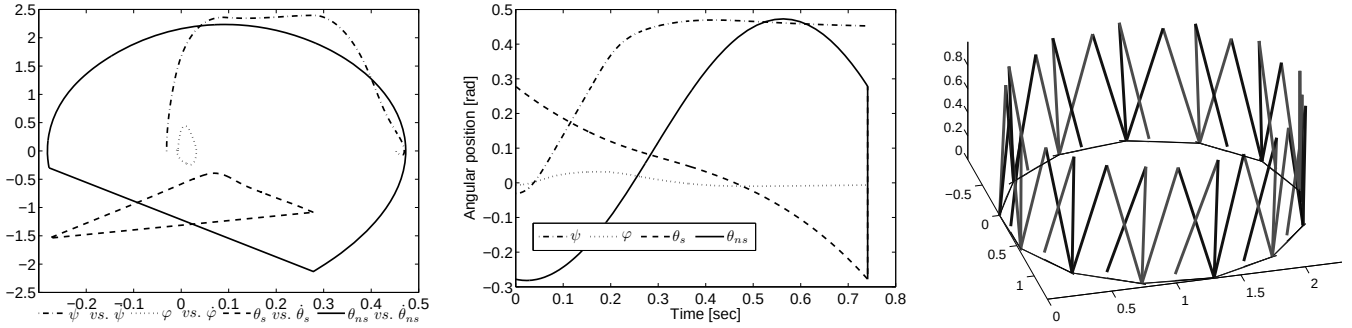

Fig. 5. Clockwise $\hat{s}$-turning 1-step gait: phase portrait (left), coordinate trajectories (center), and 13-step 360°-turn visualization (right).

gait primitives, $\{\mathcal{G}^{\mathrm{st}}, \mathcal{G}^{\mathrm{tu}(s)}, \mathcal{G}^{\mathrm{tu}(-s)}\}$, can be oriented about arbitrary headings at arbitrary times to form walking paths. Each gait has a nominal steering angle and arclength on the walking surface, but switching will result in transient variations. We must consider the stability of such transitions.

V. Sequential Composition of Primitives

We present the sequential composition of gait primitives in a manner analogous to the funneling approach of [3] and [29, Section 4.6.1]. We consider a set of dynamic gait primitives for a general biped, where we do not have an analytical/closed-form expression for the map between steps.

A biped employs[1] gait primitive $\mathcal{G}^i = (\mathscr{H}^i, x_i^*)$ during step cycle i by implementing the controller yielding closed-loop hybrid system $\mathscr{H}^i$. Gait primitives are selected at every impact event, so every step has an associated gait transition.

Definition 2: The *gait transition* of step i is defined by pair $\mathcal{T}_i = (x_i, \mathcal{G}^{i+1})$, where x_i is the state at the i^{th} impact event and $\mathcal{G}^{i+1}$ is the gait primitive during step cycle $i+1$.

[1]Turning gaits are implicity understood to be modulo steering angle s, and we assume that each gait primitive is oriented coincident with the biped's heading at the preceding gait transition.

Moreover, $\mathcal{T}_i$ is said to be *switching* if $\mathcal{G}^{i+1} \neq \mathcal{G}^i$.

Hence, $\mathcal{T}_{i+1}$ is related to $\mathcal{T}_i$ by $x_{i+1} = P_{\mathscr{H}^{i+1}}(x_i)$. And, in the case of 2-step periodic gaits, switching may only occur ever other step, implying $\mathcal{G}^{i+1} = \mathcal{G}^i$ for even i.

Definition 3: A gait transition $\mathcal{T}_i = (x_i, \mathcal{G}^{i+1})$ is *stable* if $x_i \in BoA_{\mathscr{H}^{i+1}}(x^*_{i+1})$, where $\mathscr{H}^{i+1}$ and LES fixed-point x^*_{i+1} are from gait primitive $\mathcal{G}^{i+1}$ of step cycle $i+1$.

State x_i may be the result of any gait primitive. Clearly, if $\mathcal{G}^{i+1} = \mathcal{G}^i$ and $\mathcal{T}_{i-1}$ is stable, then $\mathcal{T}_i$ is also stable. In order to determine stability for switching transitions, we first establish some properties of "nearby" gait primitives by providing numerical evidence of the following assumptions.

Assumption 1: For every $s \in [-S, S]$, there exists LES fixed-point $x^{*\mathrm{tu}(s)}$ of $P_{\mathrm{tu}(s)}$ with corresponding $BoA_{\mathrm{tu}(s)}(x^{*\mathrm{tu}(s)})$. Then, by definition there exists a non-empty open ball of radius $r_s > 0$ about $x^{*\mathrm{tu}(s)}$ such that

$$\mathcal{B}(x^{*\mathrm{tu}(s)}, r_s) \subset BoA_{\mathrm{tu}(s)}(x^{*\mathrm{tu}(s)}).$$

Moreover, assume $x^{*\mathrm{tu}(s)}$, r_s are continuous functions of s.

This is suggested by the previously discussed sampling of $[-S, S]$, shown in Fig. 4. For a sufficiently dense set of samples, input-to-state stability guarantees that state trajectories will remain nearby for steering values s between samples (arguably, such choices of s also result in unique attractive fixed-points). Furthermore, this turning motion more closely resembles straight-ahead motion for smaller steering angles:

Assumption 2: The turning fixed-point $x^{*\mathrm{tu}(s)}$ converges to straight-ahead fixed-point $x^{*\mathrm{st}} = x^{*\mathrm{tu}(0)}$ in metric space $(\mathbb{R}^{2n}, d)$ as $|s| \to 0$, where d is Euclidean distance. I.e., if $r^*_s := d(x^{*\mathrm{tu}(s)}, x^{*\mathrm{st}})$, then $\lim_{|s|\to 0} r^*_s = 0$.

Clearly, turning curvature $\kappa = \pm 1/R$ converges to straight-line curvature $\kappa = 0$ as turning radius $R \to \infty \Leftrightarrow |s| \to 0$. Thus, Assumption 2 follows from Assumption 1 by continuity. Loosely speaking, Assumption 2 implies the basins of attraction also converge, which we exploit next.

Lemma 1: Given Assumptions 1-2, there exists positive steering angle $\tilde{S} \leq S$ such that for all $s \in [-\tilde{S}, \tilde{S}]$:

1) $x^{*\mathrm{st}} \in BoA_{\mathrm{tu}(s)}(x^{*\mathrm{tu}(s)})$
2) $x^{*\mathrm{tu}(s)} \in BoA_{\mathrm{st}}(x^{*\mathrm{st}})$
3) $x^{*\mathrm{tu}(-s)} \in BoA_{\mathrm{tu}(s)}(x^{*\mathrm{tu}(s)})$

Proof: [1.1] We first define minimal ball radius $r := \min_{s\in[-S,S]}(r_s)$, positive by compactness of $[-S, S]$, so

$$\mathcal{B}(x^{*\mathrm{tu}(s)}, r) \subset \mathcal{B}(x^{*\mathrm{tu}(s)}, r_s) \subset BoA_{\mathrm{tu}(s)}(x^{*\mathrm{tu}(s)}),$$

for all $s \in [-S, S]$. Now, since $r > 0$ and $\lim_{|s|\to 0} r^*_s = 0$, $\exists\ \tilde{S} \leq S$ such that $r^*_s < r$ for all $s \in [-\tilde{S}, \tilde{S}]$. Then, $x^{*\mathrm{st}} \in \mathcal{B}(x^{*\mathrm{tu}(s)}, r)$ for all $s \in [-\tilde{S}, \tilde{S}]$, and the claim follows.

[1.2] First, by definition of LES, $\exists\ r_\infty > 0$ such that $\mathcal{B}(x^{*\mathrm{st}}, r_\infty) \subset BoA_{\mathrm{st}}(x^{*\mathrm{st}})$. Then, again $\exists\ \tilde{S}$ such that $r^*_s < r_\infty$ for all $s \in [-\tilde{S}, \tilde{S}]$. Hence, $x^{*\mathrm{tu}(s)} \in \mathcal{B}(x^{*\mathrm{st}}, r_\infty)$ for all $s \in [-\tilde{S}, \tilde{S}]$, and the claim follows.

[1.3] Recall $x^{*\mathrm{tu}(s)} \to x^{*\mathrm{st}}$ as $|s| \to 0$, which means that for each $\epsilon/2 > 0$, $\exists\ \delta > 0$ such that for all $s \in [-\delta, \delta]$, $d(x^{*\mathrm{tu}(s)}, x^{*\mathrm{st}}) < \epsilon/2$. Then, the triangle inequality shows

$$\begin{aligned} d(x^{*\mathrm{tu}(s)}, x^{*\mathrm{tu}(\text{-}s)}) &\leq d(x^{*\mathrm{tu}(s)}, x^{*\mathrm{st}}) + d(x^{*\mathrm{tu}(\text{-}s)}, x^{*\mathrm{st}}) \\ &< \epsilon \end{aligned}$$

Hence, if $r^{*\mathrm{tu}}_s := d(x^{*\mathrm{tu}(s)}, x^{*\mathrm{tu}(-s)})$, then $\lim_{s\to 0} r^{*\mathrm{tu}}_s = 0$.

Now, denoting each turning ball as $\mathcal{B}(x^{*\mathrm{tu}(s)}, r_s)$, we can define minimal ball radius $r := \min_{s\in[-S,S]}(r_s) > 0$. As we saw in 1.1, $\exists\ \tilde{S}$ such that $r^{*\mathrm{tu}}_s < r$ for all $s \in [-\tilde{S}, \tilde{S}]$. Then, $x^{*\mathrm{tu}(-s)} \in \mathcal{B}(x^{*\mathrm{tu}(s)}, r)$ for all $s \in [-\tilde{S}, \tilde{S}]$, and the claim follows. Equivalently, $x^{*\mathrm{tu}(s)} \in BoA_{\mathrm{tu}(-s)}(x^{*\mathrm{tu}(-s)})$.

Finally, we can take the minimum of $\tilde{S}$ from each proof to find $\tilde{S}$ for the overall Lemma. ■

Recall that asymptotically stability implies convergence to fixed-points in infinite time, so we show that trajectories eventually converge "close enough" to stably switch gaits.

Remark 1: Note that in Lemma 1.1, $\mathcal{B}(x^{*\mathrm{tu}(s)}, r)$ is an open ball so $x^{*\mathrm{st}}$ cannot be on the boundary of $BoA_{\mathrm{tu}(s)}(x^{*\mathrm{tu}(s)})$. Therefore, points sufficiently close to $x^{*\mathrm{st}}$ are also contained in $BoA_{\mathrm{tu}(s)}(x^{*\mathrm{tu}(s)})$. The same holds for the other three claims in Lemma 1.

Fortunately, we also have exponentially fast convergence to such neighborhoods around fixed-points. Given enough time along a given primitive, the biped's state will be "funneled" into the basin of attraction of the next primitive upon switching. This is called the *dwell time*, since the biped can be interpreted as a *discrete-time switched system* $x(i+1) = P_{\sigma(i)}(x(i))$, where switching signal $\sigma : \mathbb{Z}_+ \to \{\mathrm{st}, \mathrm{tu}(s), \mathrm{tu}(-s)\}$ chooses the primitive from step-to-step. A "supervisory" control could then constrain this signal $\sigma(\cdot)$ to stably compose gait primitives, using the following result for our switched system (cf. [1], [21] for analogous results).

Theorem 1: For any $s \in [-\tilde{S}, \tilde{S}]$ from Lemma 1, there exists a minimum number of steps $N \geq 1$, i.e., a lower bound on dwell time, such that for all integers $k \geq N$:

1) If $x \in BoA_{\mathrm{st}}(x^{*\mathrm{st}})$, then $P^k_{\mathrm{st}}(x) \in BoA_{\mathrm{tu}(s)}(x^{*\mathrm{tu}(s)})$.
2) If $x \in BoA_{\mathrm{tu}(s)}(x^{*\mathrm{tu}(s)})$, then
$$P^k_{\mathrm{tu}(s)}(x) \in BoA_{\mathrm{st}}(x^{*\mathrm{st}}).$$
3) If $x \in BoA_{\mathrm{tu}(s)}(x^{*\mathrm{tu}(s)})$, then
$$P^k_{\mathrm{tu}(s)}(x) \in BoA_{\mathrm{tu}(-s)}(x^{*\mathrm{tu}(-s)}).$$

Corollary 1: Consider primitive set $\{\mathcal{G}^{\mathrm{st}}, \mathcal{G}^{\mathrm{tu}(s)}, \mathcal{G}^{\mathrm{tu}(-s)}\}$ as in Theorem 1. For any $s \in [-\tilde{S}, \tilde{S}]$, there exists a minimum dwell time $N \geq 1$ such that for any integer $k \geq N$ the following holds: any switching transition $\mathcal{T}_{i+k}$ that follows a stable transition $\mathcal{T}_i$ is also stable.

Hence, we can piece together straight and curved gait segments, as long as the turns are not too sharp or the primitive switches too fast. The steering sharpness must be bounded by steering angle $\tilde{S}$, a condition that can be verified in simulation (checking convergence from all fixed-points). However, minimum dwell time N depends explicitly on each gait primitive's basin of attraction and rate of exponential convergence, both of which can only be characterized numerically. It may be possible to use sum-of-squares programming

to find invariant subsets of the basins of attraction [28], which would enable expressions for lower bounds on dwell time as in [1]. For the purposes of this paper, we examine our lower bound using exhaustive simulation in Section VII. We first must discuss building walking paths from gait primitives.

VI. Path Planning Formulation

Given these transition rules, we can define stable walking over a path of sequentially composed gait primitives.

Definition 4: A w-step *walking path execution* from initial condition $x(0) = x_0$ is defined by the ordered set $\mathcal{E}(x_0) = (\mathcal{T}_0, \mathcal{T}_1, \ldots, \mathcal{T}_{w-1})$, where $\mathcal{T}_0 = (x_0, \mathcal{G}^1)$.

Definition 5: A walking path execution $\mathcal{E}(x_0)$ is *robust* if all gait transitions $\mathcal{T}_i$ are stable.

In other words, the biped is guaranteed not to fall over. Recall that state x describes the robot's motion with respect to its joints. In the context of path planning, we need to consider the robot's coordinates with respect to a world frame, i.e., it's Euclidean coordinates on the walking surface. Assuming a flat surface, we need only model the biped's (x, y)-position (e.g., measured at the stance foot w.r.t. some world frame) along with heading ψ as the global orientation. Hence, every step i has an associated world configuration $c_i = (x^i_{pos}, y^i_{pos}, \psi_i)^T \in SE(2)$. The extension of a biped's discrete dynamics to coordinates $x^e_i = (x^i_{pos}, y^i_{pos}, x^T_i)^T$ is trivial, as the new coordinates are easily updated according to link angles. Through a slight abuse of notation, we denote a boundary-constrained w-step walking path execution as $\mathcal{E}^{c_w}_{c_0}(x^e_0)$, where c_0 is given by $x^e_0 = (c^T_0, \varphi_0, \theta^T_0, \dot{q}^T_0)^T$ and c_w is given by $x^e_w = P_{\mathscr{H}^w}(x^e_{w-1}) = (c^T_w, \varphi_w, \theta^T_w, \dot{q}^T_w)^T$.

We now have the framework to form paths that stably connect initial and final world configurations c_0, c_f. We can use Corollary 1 to define a class $\mathcal{C}^{c_f}_{c_0} = \left\{\mathcal{E}^{c_w}_{c_0} | c_w = c_f, w \geq 1\right\}$ of robust walking paths between reachable configurations c_0 and c_f. Moreover, our finite set of gait primitives is continuously parameterized by s to allow a (large) continuous reachable set. After encoding the transition rules into a regular language [7], walking paths can be constructed by a finite-state machine that outputs a constrained switching signal $\sigma(\cdot)$ to the biped switched system. This allows concerns of stability to be abstracted away from the planning problem.

As the biped switches between gaits, step cycle trajectories converge back and forth between attractive orbits, so we generally do not have a fixed mapping from gait transitions to path arcs. Kinodynamic planning methods (e.g., [19]) can account for these transient effects to reach precise ground configurations. Alternatively, arc characteristics can be closely estimated for each gait primitive, providing a nominal set of constant-curvature arcs for *kinematic* planning in $SE(2)$. The nominal walking paths can therefore be locally planned much like trivial Dubins curves [6]. Although ZMP biped planners often use Dubins curves as a local planning heuristic [31], our results affirm this choice from the perspective of *stability*. We defer the algorithmic and reachability details for such planning methods to future work.

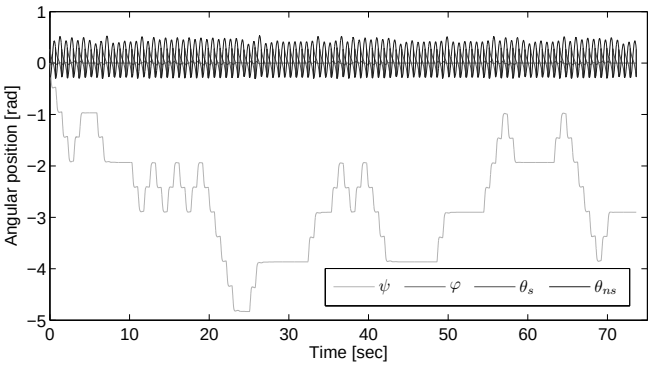

Fig. 6. Biped's random walk with gait dwell time $k = 2$ over 100 steps.

VII. Simulation Results

Although it is computationally difficult to find the exact region $[\tilde{S}, \tilde{S}]$, we can easily verify containment of a particular s through simulation. Therefore, we can confirm the conditions of Lemma 1 for primitive set $\{\mathcal{G}^{\mathrm{st}}_{4\mathrm{D}}, \mathcal{G}^{\mathrm{tu}(\hat{s})}_{4\mathrm{D}}, \mathcal{G}^{\mathrm{tu}(-\hat{s})}_{4\mathrm{D}}\}$, i.e., $\hat{s} = 0.4833 \in [\tilde{S}, \tilde{S}]$. This corresponds to

$$x^{*\mathrm{st}}_{4\mathrm{D}}, x^{*\mathrm{tu}(\hat{s})}_{4\mathrm{D}}, x^{*\mathrm{tu}(-\hat{s})}_{4\mathrm{D}} \in BoA_{\mathrm{st}} \bigcap BoA_{\mathrm{tu}(\hat{s})} \bigcap BoA_{\mathrm{tu}(-\hat{s})}.$$

This overlapping attractive region influences the minimum dwell time N along gaits for Theorem 1. We simulate worst-case gait switching tests to deduce N for this primitive set.

Based on the intuition provided by Theorem 1, worst-case walking scenarios are those with the highest frequencies of switching gait transitions (i.e., dwell time $k < N$). The more often a biped switches between gait primitives, the more likely it will accumulate transient perturbations that cannot be attenuated during the short duration of each primitive. Eventually, the impact-event state from one gait primitive will be outside the basin of attraction of the next.

We first simulate switching between two fixed gaits at every step (i.e., $k = 1$). Both the CW-to-CCW and CW-to-Straight cases eventually converge to 2- and 4-periodic cycles, respectively, showing that the biped is robust for periodic switching transitions. We next try a "random walk," randomly picking a gait primitive from a uniform distribution at every step. Here, we observe occasional falls, e.g., the sequence (CW,S,S,S,CW,S,S,S), implying that $N > 1$. Setting $k = 2$ (switching allowed every other step), we are unable to produce falls after several lengthy simulations (100+ steps, e.g., Fig. 6), suggesting that minimum dwell time $N = 2$.

This is evidence that the overlapping attractive region of our primitive set is large. This is due to the close proximity of the set's fixed-points, e.g., $d(x^{*\mathrm{tu}(\hat{s})}_{4\mathrm{D}}, x^{*\mathrm{tu}(-\hat{s})}_{4\mathrm{D}}) < 0.064$, as well as the large size of each gait's basin of attraction. This shows that our primitive set is capable of building a large class of robust walking paths, enabling path planning through 3-D space as in the obstacle avoidance example of Fig. 7. Integrating $\dot{q}^T u$ to obtain net work per step, the specific *mechanical* cost of transport for each gait is $c^{*\mathrm{st}}_{mt} = 0.052$ and $c^{*\mathrm{tu}(\pm\hat{s})}_{mt} = 0.06$, which compares favorably against the Cornell biped at $c_{mt} = 0.055$ and ASIMO at $c_{mt} = 1.6$ [4].

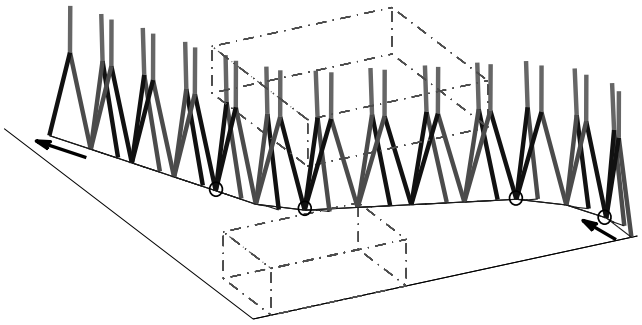

Fig. 7. Example of a planned path using gait primitives for a torso biped. The sequence of primitives is (S, CCW, CCW, S, S, S, S, CW, CW, S, S, S, S), where switching transitions are signified by circles at the impact events.

VIII. Conclusions

The planning framework of dynamic gait primitives can be used with any control method that produces asymptotic stable walking (e.g., [11], [25]). Each gait primitive is characterized by its hybrid system dynamics and stable fixed-point, thus corresponding to a nominal hybrid periodic orbit. In our compass-gait example, these orbits are naturally attractive by the (pseudo-passive) robot dynamics after controlled reduction. Simulations show that the biped stably switches gaits for dwell times $k \geq 2$, which affords significant maneuverability.

This motion is not prescribed by full-state trajectories [7] or subjected to any postural constraints to ensure stability [12], [15], yet we have deduced robustness over a *large* class of paths composed of gait primitives. This allows decomposed *kinematic* planning for *fast* and *efficient* bipedal locomotion based on human-like passive walking principles, which is fundamentally different from ZMP methods. Future work will detail high-level planning algorithms that can integrate a suite of other motion control tools for dynamic walkers, such as step-level planning over rough terrain [22], [24] and time-scaling for variable walking speeds [14]. Experimental results have been achieved for planar limit cycle walking (cf. [29]), and 3-D results may soon be possible with advances in actuator and biped mechanical design.

The turning gaits in this paper exhibit the sagittal-plane periodicity of straight-ahead gaits with slight step length and velocity adjustments, as in the human turning studies of [5]. This begs interesting questions about the existence of motion primitives in human locomotor control based on the spinal cord's central pattern generator, which we leave to the reader.

Acknowledgments

We thank Jessy W. Grizzle, Nikolaos Freris, Daniel Liberzon, and Tansu Alpcan for their many helpful comments.

References

[1] T. Alpcan and T. Basar, "A stability result for switched systems with multiple equilibria," *Dynamics of Continuous, Discrete and Impulsive Systems*, 2009, under review.

[2] A. D. Ames, R. D. Gregg, and M. W. Spong, "A geometric approach to three-dimensional hipped bipedal robotic walking," in *Conf. on Decision and Control*, New Orleans, LA, 2007.

[3] R. Burridge, A. Rizzi, and D. Koditschek, "Sequential composition of dynamically dexterous robot behaviors," *Int. J. of Robotics Res.*, vol. 18, no. 6, pp. 534–555, 1999.

[4] S. H. Collins and A. Ruina, "A bipedal walking robot with efficient and human-like gait," in *Int. Conf. on Robotics and Automation*, Barcelona, Spain, 2005.

[5] G. Courtine and M. Schieppati, "Human walking along a curved path. I. body trajectory, segment orientation and the effect of vision," *European J. of Neuroscience*, vol. 18, no. 1, pp. 177–190, 2003.

[6] L. E. Dubins, "On curves of minimal length with a constraint on average curvature, and with prescribed initial and terminal positions and tangents," *Amer. J. of Math.*, vol. 79, no. 3, pp. 497–516, 1957.

[7] E. Frazzoli, M. A. Dahleh, and E. Feron, "Maneuver-based motion planning for nonlinear systems with symmetries," *IEEE Trans. on Robotics*, vol. 21, no. 6, pp. 1077–1091, 2005.

[8] A. Goswami, B. Thuilot, and B. Espiau, "Compass-like biped robot part I: Stability and bifurcation of passive gaits," Institut National de Recherche en Informatique et en Automatique, Tech. Rep. 2996, 1996.

[9] R. D. Gregg and M. W. Spong, "Bringing the compass-gait bipedal walker to three dimensions," in *Int. Conf. on Intelligent Robots and Systems*, St. Louis, MO, 2009.

[10] ——, "Reduction-based control of branched chains: Application to three-dimensional bipedal torso robots," in *Conf. on Decision and Control*, Shanghai, China, 2009.

[11] ——, "Reduction-based control of three-dimensional bipedal walking robots," *Int. J. of Robotics Res.*, Accepted 2009, pre-print.

[12] K. Hauser, T. Bretl, J.-C. Latombe, K. Harada, and B. Wilcox, "Motion planning for legged robots on varied terrain," *Int. J. of Robotics Res.*, vol. 27, no. 11-12, pp. 1325–1349, 2008.

[13] D. Hobbelen and M. Wisse, "Limit cycle walking," in *Humanoid Robots: Human-like Machines*. Vienna, Austria: I-TECH, 2007.

[14] J. K. Holm, D. Lee, and M. W. Spong, "Time-scaling trajectories of passive-dynamic bipedal robots," in *Int. Conf. on Robotics and Automation*, Roma, Italy, 2007.

[15] J. Kuffner, K. Nishiwaki, S. Kagami, M. Inaba, and H. Inoue, "Motion planning for humanoid robots," in *Robotics Research*. Springer, 2005.

[16] J. J. Kuffner-Jr., S. Kagami, K. Nishiwaki, M. Inaba, and H. Inoue, "Dynamically-stable motion planning for humanoid robots," *Autonomous Robots*, vol. 1, no. 12, pp. 105–118, 2002.

[17] A. D. Kuo, "Stabilization of lateral motion in passive dynamic walking," *Int. J. of Robotics Res.*, vol. 18, no. 9, pp. 917–930, 1999.

[18] ——, "Choosing your steps carefully: walking and running robots," *IEEE Robotics and Automation Mag.*, vol. 14, no. 2, pp. 18–29, 2007.

[19] S. M. LaValle and J. J. Kuffner-Jr., "Randomized kinodynamic planning," *Int. J. of Robotics Res.*, vol. 20, no. 5, pp. 378–400, 2001.

[20] W. R. Leonard and M. L. Robertson, "Energetic efficiency of human bipedality," *Amer. J. of Phys. Anthro.*, vol. 97, pp. 335–338, 1995.

[21] D. Liberzon, *Switching in Systems and Control*. Springer, 2003.

[22] I. R. Manchester, U. Mettin, F. Iida, and R. Tedrake, "Stable dynamic walking over rough terrain: Theory and experiment," *Int. Symp. on Robotics Research*, 2009.

[23] T. McGeer, "Passive dynamic walking," *Int. J. of Robotics Res.*, vol. 9, no. 2, pp. 62–82, 1990.

[24] S. Ramamoorthy and B. Kuipers, "Trajectory generation for dynamic bipedal walking through qualitative model based manifold learning," in *Int. Conf. on Robotics and Automation*, 2008, pp. 359–366.

[25] C. Shih, J. W. Grizzle, and C. Chevallereau, "From stable walking to steering of a 3D bipedal robot with passive point feet," *IEEE Trans. Systems, Man, and Cybernetics, B*, 2009, under review.

[26] R. Sinnet and A. D. Ames, "3D bipedal walking with knees and feet: A hybrid geometric approach," in *Conf. on Decision and Control*, Shanghai, China, 2009.

[27] K. Steudel, "Limb morphology, bipedal gait, and the energetics of hominid locomotion," *Amer. J. of Phys. Anthro.*, vol. 99, 1996.

[28] U. Topcu, A. Packard, and P. Seiler, "Local stability analysis using simulations and sum-of-squares programming," *Automatica*, vol. 44, no. 10, pp. 2669–2675, 2008.

[29] E. R. Westervelt, J. W. Grizzle, C. Chevallereau, J. H. Choi, and B. Morris, *Feedback Control of Dynamic Bipedal Robot Locomotion*. New York, New York: CRC Press, 2007.

[30] Wikipedia, 2006, http://en.wikipedia.org/wiki/Sagittal_plane.

[31] E. Yoshida, C. Esteves, I. Belousov, J.-P. Laumond, T. Sakaguchi, and K. Yokoi, "Planning 3-D collision-free dynamic robotic motion through iterative reshaping," *IEEE Trans. on Robotics*, vol. 24, no. 5, pp. 1186–1198, 2008.